Med Chem Res
DOI 10.1007/s00044-016-1597-8

MEDICINAL CHEMISTRY RESEARCH

ORIGINAL RESEARCH

Synthesis, anticonvulsant activity and QSAR studies of some new pyrazolyl pyridines

Joohee Pradhan[1,2] · **Anju Goyal**[3]

Received: 22 December 2015 / Accepted: 10 May 2016

Abstract Twenty-one new 3,5-bipyridinyl-1*H*-pyrazole derivatives (pyrazolyl pyridines) have been synthesized and evaluated for their anticonvulsant activity in animal models of epilepsy. The pyrazolyl pyridines, **7–27**, were obtained through a general one-pot synthesis, from ketones and acid chlorides via formation of 1,3-diketones in situ carried out in hydrocarbon solvent and LiHMDS base. The profile of anticonvulsant activity of final compounds was established in the maximal electroshock (MES) and subcutaneous pentylenetetrazole (sc PTZ) tests, after intraperitoneal injection in rats and mice, respectively, at doses of 30, 100, and 300 mg/kg. An observation was carried out at two different time intervals—0.5 and 4 h. Phenytoin was used as a standard antiepileptic against MES convulsions and valproic acid against sc PTZ convulsions. Furthermore, in addition to the primary anticonvulsant screening, the acute neurological toxicity was determined in mice by the rotarod test and in rats by positional sense test. The compounds showed anticonvulsant activity exclusively against MES convulsions. The compounds were found especially active in 100 mg/kg dose at both the time points, i.e., 0.5 and 4 h, depending upon the lipophilicity of molecules as indicated by statistically significant reduction in the time spent in tonic extension phase ($p < 0.001$). Further, the newly synthesized compounds were subjected to two-dimensional quantitative structure–activity relationship (2D QSAR) analysis through multiple linear regression, principal component regression, and partial least square regression analysis, and three-dimensional quantitative structure–activity relationship (3D QSAR) analysis by k-nearest neighbor molecular field analysis in conjunction with stepwise forward–backward, genetic algorithm, and simulated annealing variable selection methods using the software VLife MDS. The structure–activity relationship (SAR) as well as quantitative structure–activity relationship (QSAR) studies for anticonvulsant activity confirmed the crucial role of 3,5-bipyridinyl-1*H*-pyrazole core fragment for anticonvulsant activity.

Keywords Pyrazolyl pyridines · Anticonvulsant · SAR · 2D QSAR · 3D QSAR · KNN-MFA

Introduction

Epilepsy is the commonest neurological condition affecting people of all ages, race, and social class. There are 50 million people living with epilepsy worldwide, and most of them reside in developing countries. About 10 million persons with epilepsy are there in India. Many people with active epilepsy do not receive appropriate treatment for their condition, leading to large treatment gap (Subbareddy *et al.*, 2014). Over the years, the field of epilepsy has received a great deal of attention from research investigators in the hope of discovering new drugs that are more effective and have minimal adverse effects. Though several new anticonvulsants have been introduced, some types of epilepsies are still not adequately controlled with the current therapy. Adverse reactions and lack of efficacy for

✉ Joohee Pradhan
juhipradhan123@gmail.com

[1] Department of Pharmaceutical Sciences, Mohanlal Sukhadia University, Udaipur, Rajasthan 313001, India

[2] Pacific Academy of Higher Education and Research University, Pacific Hills, Udaipur, Rajasthan 313001, India

[3] B. N. Institute of Pharmaceutical Sciences, Sewashram Road, Udaipur, Rajasthan 313001, India

Published online: 28 May 2016

certain types of epilepsies are some of the limitations of existing medications (Löscher and Schmidt 2002). Taking into consideration the above limitations, many authors conducted attempts to identify the structural features crucial for anticonvulsant activity. On the basis of these researches, several pharmacophoric models, enabling a more rational design of new anticonvulsants, have been described. Thus, one of the important core fragments of anticonvulsants is defined by nitrogen heterocyclic system, usually imide or lactam and phenyl or alkyl groups attached to the heterocyclic system (Wong *et al.*, 1986; Bruno-Blanch *et al.*, 2003; Malawska, 2005). This common template is present in the structures of old, however well-established antiepileptic drugs (AEDs), such as ethosuximide and phenytoin as well as among the newest drugs, e.g., levetiracetam, brivaracetam, or seletracetam (Rogawski and Porter, 1990; Bialer *et al.*, 2007). Bearing in mind the aforementioned, we have synthesized in our laboratory a series of 3,5-bipyridinyl-1*H*-pyrazole derivatives differently substituted at the 2-position of both the pyridine rings, as candidates for new AEDs.

Marketed AEDs predominantly target voltage-gated cation channels (the α-subunits of voltage-gated Na^+ channels and also T-type voltage-gated Ca^{2+} channels) or influence GABA-mediated inhibition. Recently, $\alpha 2-\delta$ voltage-gated Ca^{2+} channel subunits and the SV2A synaptic vesicle protein have been recognized as likely targets (Meldrum and Rogawski, 2007). Voltage-gated Na^+ channels are essential for action potentials, and their mutations are the substrate for generalized epilepsy with febrile seizures plus and benign familial neonatal infantile seizures; Na^+ channel inhibition is the primary mechanism of carbamazepine, phenytoin, and lamotrigine and is a probable mechanism for many other classic and novel AEDs (Armijo *et al.*, 2005). Most of the older anticonvulsants have close structural similarity. This is depicted in Fig. 1. The structural similarity of newly synthesized pyrazolyl pyridines to established anticonvulsant drugs, especially Hydantoin derivatives (e.g., phenytoin) in having five-membered heterocyclic systems with two nitrogen atoms, gives rise to the possibility of Na^+ channel inhibition as the most probable mechanism of action of these compounds.

Quantitative structure–activity relationships (QSAR), as a major factor in drug design, are mathematical equations relating chemical structure to their biological activity (Krogsgaard-Larsen *et al.*, 2002). Anticonvulsant agents have been the aim of many SAR and QSAR studies (Palluotto *et al.*, 1996; Marone *et al.*, 1999; Hou and Xu, 2001; Marder *et al.*, 2001; Verli *et al.*, 2002). Palludotto *et al.* (1996) synthesized a series of 2-aryl-2,5-dihydropyridazino[4,3-b]indol-3-one derivatives and tested them as central benzodiazepine receptor ligands. These workers used 2D and 3D QSAR on these molecules and observed that the molar refractivity (MR) of the substituents was the major factor controlling the binding of the ligands to their receptors. A correlation between the theoretical descriptors of the tricyclic neuroactive drugs and their biological mode of action has been obtained by the theoretical studies of Marone and coworkers (Marone *et al.*, 1999). Three-dimensional QSAR analyses on the anticonvulsant activity of a series of cinnamamides using comparative molecular field analysis (CoMFA) and comparative molecular similarity indices analysis (CoMSIA) approaches have been reported by Hou and Xu (2001). These investigators found that the interaction of these compounds with receptors is achieved by electrostatic and hydrophobic forces. Marder *et al.* (2001) have reported molecular modeling and QSAR analysis of flavone derivatives upon interaction with benzodiazepine binding site. The electronic properties of the ligands were found to be the major factor affecting the ligand–receptor binding (Verli *et al.*, 2002). VLife Molecular Design Suite (VLife MDS; Supplied by VLife Science technologies, Pune, India.) is a medicinal chemist's work bench for Computer-Aided Drug Design and molecular discovery. VLife MDS is completely scalable and customizable to address the variegated problems in molecular design and prediction of new molecules. VLife MDS facilitates comprehensive in silico approach to design, visualize, predict, and analyze the small molecules as well as proteins and study their interactions. Among its various applications, molecular modeling, energy minimization, geometry optimization, and 2D QSAR and 3D QSAR by k-nearest neighbor molecular field analysis (KNN-MFA) studies were used for the present study. KNN-MFA (Ajmani *et al.*, 2006) requires suitable alignment of given set of molecules. This is

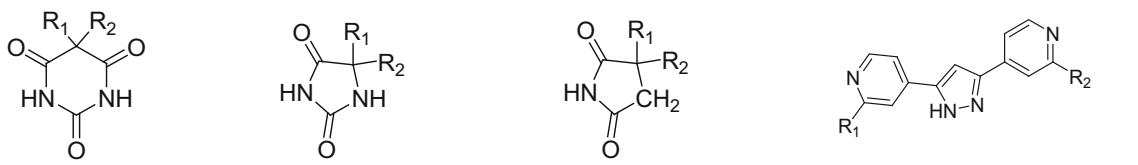

Fig. 1 Structural similarity of established anticonvulsant drugs with that of synthesized compounds

followed by generation of a common rectangular grid around the molecules. The steric and electrostatic interaction energies are computed at the lattice points of the grid using a methyl probe of charge +1. These interaction energy values are considered for relationship generation and utilized as descriptors to decide nearness between molecules. The term descriptor is utilized in the following discussion to indicate field values at the lattice points. The optimal training and test sets were generated using the sphere exclusion algorithm. This algorithm allows the construction of training sets covering descriptor space occupied by representative points. Once the training and test sets were generated, KNN methodology was applied to the descriptors generated over the grid.

In the present study, we report the synthesis, anticonvulsant evaluation, and QSAR studies of new pyrazolyl pyridines to be considered as a template for the development of new, potential anticonvulsant agents in future.

Results and discussion

Chemistry

The title compounds pyrazolyl pyridines **7–27** (Table 1) were synthesized from methyl pyridyl ketones (**1a–6a**) and pyridyl acid chlorides (**1b–6b**) according to the scheme (Fig. 2), where, as shown in Fig. 3, 1,3-diketones were synthesized directly from ketones and acid chlorides and were then converted in situ into pyrazoles by the addition of hydrazine hydrate. This method was proved to be extremely fast, general, and chemoselective. The reaction was carried out under the atmosphere of nitrogen, in a hydrocarbon solvent, so as to suppress the side reactions by disfavoring a charged intermediate, only allowing the enolate to react with the very electrophilic acid chloride. LiHMDS was found to be the base of choice because as reported previously (Heller and Natarajan, 2006), it does

Table 1 List of synthesized compounds **7–27**

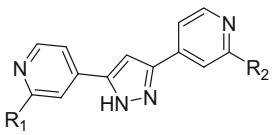

Sl. no.	Compound ID	R_1	R_2
1.	**7.**	–H	–H
2.	**8.**	$–NO_2$	–H
3.	**9.**	$–NH_2$	–H
4.	**10.**	–Cl	–H
5.	**11.**	$–C_6H_5$	–H
6.	**12.**	$–C_6H_4CH_3$	–H
7.	**13.**	$–NO_2$	$–NO_2$
8.	**14.**	$–NH_2$	$–NH_2$
9.	**15.**	–Cl	–Cl
10.	**16.**	$–C_6H_5$	$–C_6H_5$
11.	**17.**	$–C_6H_4CH_3$	$–C_6H_4CH_3$
12.	**18.**	–Cl	$–NO_2$
13.	**19.**	–Cl	$–NH_2$
14.	**20.**	–Cl	$–C_6H_5$
15.	**21.**	–Cl	$–C_6H_4CH_3$
16.	**22.**	$–NO_2$	$–NH_2$
17.	**23.**	$–NO_2$	$–C_6H_5$
18.	**24.**	$–NO_2$	$–C_6H_4CH_3$
19.	**25.**	$–NH_2$	$–C_6H_5$
20.	**26.**	$–NH_2$	$–C_6H_4CH_3$
21.	**27.**	$–C_6H_5$	$–C_6H_4CH_3$

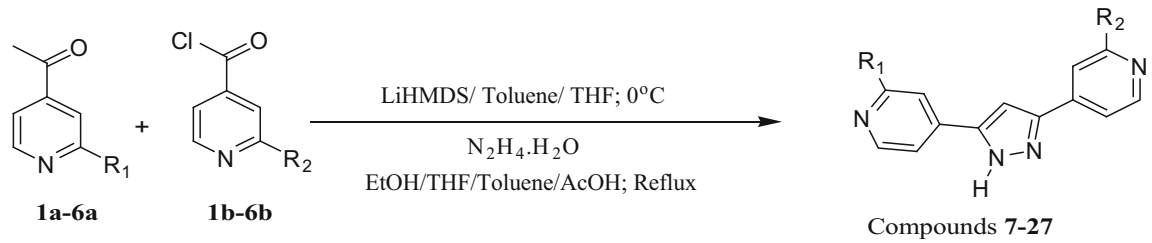

Fig. 2 Scheme for the synthesis of title compounds **7–27**

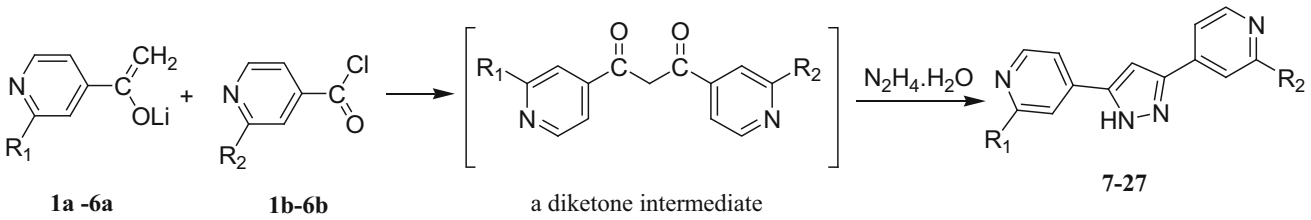

Fig. 3 Synthesis of title compounds through 1,3-diketone intermediate

not give an additional triketone intermediate as with the use of other bases like NaHMDS or KHMDS, arising from a metal diketone reacting with another equivalent of acid chloride.

Different ketones were prepared from 4-acetyl pyridine or methyl pyridyl ketones by substitution at position 2-via N-oxide intermediate as reported by us previously (Pradhan and Goyal, 2015). Likewise, different acid chlorides used were isonicotinoyl chloride and derivatives of isonicotinoyl chloride prepared from ethyl isonicotinate via N-oxide intermediate. Ethyl group acted as protecting group which later on converted via alkaline hydrolysis to parent acid after substitution at position 2. The acid so obtained was then converted to acyl chloride by thionyl chloride. The N-oxides in both the above cases were reduced back to the base by palladium and carbon in ethyl formate and methanol. The final compounds were fully characterized by elemental analyses (C, H, N) and ^{1}H NMR, ^{13}C NMR, LC/MS spectra. The detailed physicochemical and analytical data are listed in the experimental section. The structures of intermediates **1a–6a** and **1b–6b** are given in Table 2.

IR spectrum of the compounds in general showed heteroaromatic C–H stretching vibrations between 3000 and 3100 cm^{-1}, =C–N str. for pyridines at about 1250 cm^{-1}; 2° N–H str. in pyrazole between 3100 and 3500 cm^{-1}, C=N str. at about 1650 cm^{-1}, aromatic C=C str. between 1400 and 1700 cm^{-1} and N–H bend at about 1200 cm^{-1}. ^{1}H NMR spectrum of the compounds in general showed signal for aromatic protons between δ 6.3 and 8.5 ppm as multiplet. A sharp singlet formed between δ 9.85 and 10.62 ppm was attributed to the N–H proton. IR spectrum of compounds **8**, **13**, **18**, **22**, **23**, and **24** showed two bands at about 1000 and 1400 cm^{-1}, respectively, due to symmetrical N=O stretch which confirms the presence of nitro group in these compounds. Compounds **9**, **14**, **19**, **22**, **25**, and **26** showed two IR stretching vibrational bands at about 3405 and 3382 cm^{-1} attributed to N–H str. in primary aromatic amines. Further, a sharp singlet at δ 1.43 ppm in ^{1}H NMR spectrum of these compounds showed the presence of two protons of NH_2 group. Compound nos. **15**, **18**, **19**, **20**, and **21** containing chloro substitutions showed an IR band at about 745–677 cm^{-1} attributed to C–Cl str. in aromatic halogen compounds. A proton NMR signal of the same compounds between δ 3.3–4.8 ppm indicates the proton attached to the carbon-containing halogen atom. Compound nos. **11**, **16**, **20**, **23**, **25,** and **27** contained more intense C–H stretching vibrational band at about 3040 cm^{-1}, indicating the quantitative relationship between number of aromatic C–H bonds and intensity of IR bands. Compounds **12**, **17**, **21**, **24**, **26**, and **27** containing tolyl substituents on pyridine ring showed additional aliphatic Sp^3 C–H stretching vibration at 2872–3178 cm^{-1}. Further, ^{1}H NMR spectrum of these compounds showed a signal at δ 0.5–1.5 ppm which confirms the presence of simple Sp^3 C–H in the compounds. The ^{13}C NMR spectrum of all the compounds in general showed three peaks at about δ 147.18, 146.18, and 103.52 ppm which correspond to carbon atoms of pyrazole ring. The carbon atom of the methyl group at the tolyl fragment occurred as peak at δ 21.13 ppm. The peaks of carbon atoms of the aromatic rings were detected at the expected chemical shifts within the range δ 111–160 ppm. The molecular formulae of the synthesized compounds **7–27** were confirmed by elemental analysis. Elemental analysis was carried out for carbon, hydrogen, and nitrogen. The results obtained were within ±0.4 % of

Table 2 Intermediates for the synthesis of compounds **7–27**

Intermediate code	Structure	Intermediate code	Structure
1a	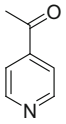 1-(pyridin-4-yl)ethanone	**1b**	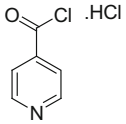 isonicotinoyl chloride hydrochloride
2a	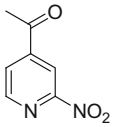 1-(2-nitropyridin-4-yl)ethanone	**2b**	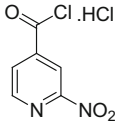 2-nitropyridine-4-carbonyl chloride hydrochloride
3a	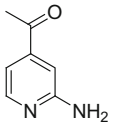 1-(2-aminopyridin-4-yl)ethanone	**3b**	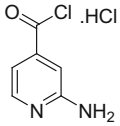 2-aminopyridine-4-carbonyl chloride hydrochloride
4a	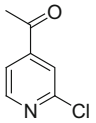 1-(2-chloropyridin-4-yl)ethanone	**4b**	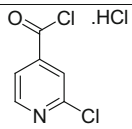 2-chloropyridine-4-carbonyl chloride hydrochloride
5a	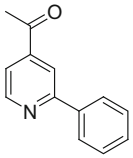 1-(2-phenylpyridin-4-yl)ethanone	**5b**	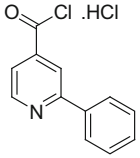 2-phenylpyridine-4-carbonyl chloride hydrochloride
6a	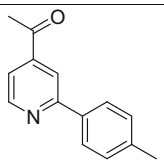 1-(2-p-tolylpyridin-4-yl)ethanone	**6b**	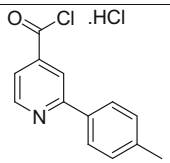 2-p-tolylpyridine-4-carbonyl chloride hydrochloride

the theoretical value. The molecular weight of the compounds was confirmed by mass spectroscopy. The molecular ion peaks obtained were in good agreement with the molecular weight of the compounds. All the synthesized compounds **7–27** exhibited satisfactory spectral data consistent with their structure.

Anticonvulsant activity

The profile of anticonvulsant activity of final compounds **7**–**27** was established in the MES and scPTZ tests, after intraperitoneal (i.p.) injection in rats and mice, respectively, at doses of 30, 100, and 300 mg/kg. An observation was carried out at two different time intervals—0.5 and 4 h. Furthermore, in addition to the primary anticonvulsant screening, the acute neurological toxicity (NT) was determined in mice by the rotarod test and in rats by positional sense test. The results of the preliminary pharmacological studies are summarized in Table 3.

The compounds tested showed protection exclusively in the MES seizures. Furthermore, in vivo data revealed that anticonvulsant activity was closely connected with the type of substituent at the pyridine moiety in the present pyrazolyl pyridines. Among all the synthesized compounds, compound nos. **7**, **8**, **9**, **10**, **14**, **18**, and **19** having substitution –H, $–NO_2$, $–NH_2$, or –Cl at R_1 position were found to be the most active compounds (i.e., compounds effective in a dose of 100 mg/kg at 0.5 h) which indicated that as compared with other compounds in the series, a less bulky substituent with variable electronic character favors the anticonvulsant activity of these compounds against MES convulsions. The aforementioned active compounds have R_2 substitution as either –H, $–NH_2$, or $–NO_2$. Here, it is noteworthy that no compound with –Cl substitution at $–R_2$ was active at 0.5 h in 100 mg/kg dose, but the criterion of variable electronic character at R_2 remains the same as with R_1. Thus, by observing the SAR of active compounds, it is imperative to say that bulk, but not the electronic character of the substituent is important at both R_1 and R_2 position of the compounds with the remark that –Cl substitution at R_2 is not important for anticonvulsant activity. These observations indicate that receptor site may allow only less bulky, smaller compound to interact with it, with little electronic interactions; however, along with the bulk, polarity as well as the electronegativity of the substituents turned out to be important and decided the activity of the compounds depending upon the position on the molecule where they are attached. This has been proved through QSAR study in the coming sections. Compounds **11**, **12**, **15**, **20**, **23**, **24**, **25**, and **26** showed protection for MES seizures only 4 h after i.p. administration that means delayed onset, however long duration of anticonvulsant action of these compounds. As compared with the most active compounds, these compounds had bulkier substitution either at R_1 (comp. nos. **11** and **12**) or at R_2 (comp. nos. **20**, **23**, **24**, **25**, and **26**) position; an exception to this was compound **15** having $R_1 = R_2 =$ Cl which indicated that although less bulky, -chloro substitution at both the positions was responsible for delayed action. Additionally, compounds **13**, **16**, **17**, **21**, **22**, and **27** showed no anticonvulsant activity in all the tested doses at any time interval. This indicated that bulky substitution ($–C_6H_4CH_3$) at R_2 is detrimental for the said activity, but when combined with $–NO_2$ or $–NH_2$, as in compounds **21** and **26**, respectively, increased potency as well as toxicity of the compounds. The major group responsible for respiratory depression in rats seemed to be $–C_6H_4CH_3$, coupled with –H or NO_2 as observed during pharmacological screening of compounds **12** and **24**. Compound **20** with –Cl and $–C_6H_5$ substitution at R_1 and R_2, respectively, caused tremors in rats at 300 mg/kg dose. Good anticonvulsant activity of compound **7** at 100 mg/kg and no activity of compound **27** at all three doses indicated that the nucleus 3,5-bipyridinyl-1*H*-pyrazole itself is crucial for anticonvulsant activity and the bulky substitution on the nucleus is detrimental for the activity.

The differences in times points in which the anticonvulsant protection was observed for compounds containing pyrazolyl pyridine nucleus may result from the lipophilic properties of these molecules. As it is presented in Table 3, the more lipophilic molecules (higher clog *P* values)—**11**, **12**, **15**, **20**, **23**, **24**, **25**, and **26**—showed activity mainly at 4 h, whereas less lipophilic compounds—**7**, **8**, **9**, **10**, **14**, **18**, and **19—**were effective only at time point of 0.5 h. These observations may be connected with higher affinity of more lipophilic compounds to the peripheral tissues that causes slower distribution to the CNS. Further, inactivity of compounds **16**, **17**, **20**, and **27** against MES seizures supported the Lipinski's rule of 5 which says that a drug having log *P* value greater than 5 would not have good absorption properties, so will not be a good choice as a drug. Most CNS active drugs have log *p* less than 5 so it is easily absorbed in blood–brain barrier where active diffusion of drug is likely to have most lipophilic area like lipid bilayer of membrane, and if the value is less than 0, it will move toward hydrophilic compartment like blood serum (Lien *et al.*, 1973).

The overall SAR analysis indicated that pyrazolyl pyridines with less bulky substituent of variable electronic character at R_1 were therapeutically active as well as less toxic while bulkier substitution at R_2 as in compounds **20**, **24**, and **26** caused neurotoxicity. Good anticonvulsant activity of compound **7** indicated the crucial role of the nucleus 3,5-bipydidinyl-*1H*-pyrazole for antiepileptic activity. -Chloro substituent, when attached to R_1, was favorable for anticonvulsant activity as exemplified by compounds **10**, **15**, **18**, **19**, and **20**, but when attached to R_2 (comp. **15**), it caused delayed onset of action. The nucleus itself was found to be a good anticonvulsant. Accordingly, seven best compounds with anticonvulsant activity were **7**, **8**, **9**, **10**, **14**, **18**, and **19**; all these compounds showed no

Table 3 Anticonvulsant activity of compounds **7–27** after i.p. administration in rats/mice

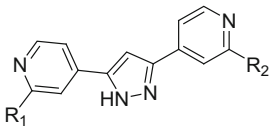

Treatment (comp. no.)	R_1	R2	Intraperitoneal administration in rats/mice[a]						CLogP[e]
			MES[b]		scPTZ[c]		NT[d]		
			0.5 h	4 h	0.5 h	4 h	0.5 h	h	
7.	–H	–H	100	–	–	–	–	–	1.7037
8.	$–NO_2$	–H	100	–	–	–	–	–	1.62028
9.	$–NH_2$	–H	100	–	–	–	–	–	1.38979
10.	–Cl	–H	100	–	–	–	–	–	2.4924
11.	$–C_6H_5$	–H	–	100	–	–	–	–	3.8017
12.	$–C_6H_4CH_3$	–H	–	100	–	–	300[z]		4.3007
13.	$–NO_2$	$–NO_2$	–	–	–	–	–	–	1.51137
14.	$–NH_2$	$–NH_2$	100	–	–	–	–	–	1.06672
15.	–Cl	–Cl	–	100	–	–	–	–	3.25683
16.	$–C_6H_5$	$–C_6H_5$	–	–	–	–	–	–	5.8997
17.	$–C_6H_4CH_3$	$–C_6H_4CH_3$	–	–	–	–	–	–	6.8977
18.	–Cl	$–NO_2$	100	–	–	–	–	–	2.38471
19.	–Cl	$–NH_2$	100	–	–	–	–	–	2.17849
20.	–Cl	$–C_6H_5$	–	100	–	–	300[y]	–	4.5904
21.	–Cl	$–C_6H_4CH_3$	–	–	–	–		–	5.0662
22.	$–NO_2$	$–NH_2$	–		–	–	–	–	1.30637
23.	$–NO_2$	$–C_6H_5$	–	100	–	–	–	–	3.71828
24.	$–NO_2$	$–C_6H_4CH_3$	300	100	–	–	300[z]	–	4.19408
25.	$–NH_2$	$–C_6H_5$	–	100	–	–	–	–	3.48779
26.	$–NH_2$	$–C_6H_4CH_3$	300	100	–	–	300	–	3.98679
27.	$–C_6H_5$	$–C_6H_4CH_3$	–	–	–	–	–	–	6.3987
Phenytoin[f]			30	30	–	–	100	100	2.605
Valproic acid[f]			–	–	300	300	–	–	2.75

Response comments: [z]respiratory depression, [y]tremors

[a] Doses of 30, 100, or 300 mg/kg were administered intraperitoneally in rats for MES test and in mice for scPTZ test. The data indicate the minimum dose effective or neurotoxic in half or more animals tested. A dash indicates the absence of anticonvulsant activity or neurotoxicity at the maximum dose administered

[b] Maximal electroshock test

[c] Subcutaneous pentylenetetrazole test

[d] Neurotoxicity screening using rotarod test

[e] clog *P* values calculated using a log *P* module of ChemDraw Ultra program, version 7.0.1 (Cambridge Soft Corporation, Cambridge, MA, USA)

[f] Phenytoin and valproic acid, reference antiepileptic drugs tested by use of ADD Program procedures in NIH/NINDS

neurotoxicity in the highest dose tested and can be subjected to sodium channel binding assay for the determination of their mechanism of action. Thus, these compounds may be useful for future development of anticonvulsant drugs for grand mal epilepsy.

QSAR study

An intensive 2D QSAR study of 21 compounds (divided into 7 test and 14 training sets) for anticonvulsant activity against MES convulsions was carried out through multiple

linear regression (MLR), principal component regression (PCR), and partial least square (PLS) regression analysis using VLife MDS. The most statistically significant model obtained through PCR is presented below:

$$-\log(\%\ \text{inhibition}) = +0.1148(\pm 0.0271)\text{T\_T\_N\_3} - 0.0648(\pm 0.0204)\text{SK MostHydrophobic Hydrophilic Distance} - 2.4069$$

$n = 14$	r^2_se = 0.2042
Degree_of_freedom = 11	q^2_se = 0.2579
$r^2 = 0.6384$	pred_r^2 = 0.5452
$q^2 = 0.5227$	pred_r^2se = 0.2987
F_test = 9.7083	

The equation explains 63 % ($r^2 = 0.6384$) of the total variance in the training set. It also has an internal (q^2) and external (pred_r^2) predictive ability of ~52 and ~54 %, respectively. The F-test = 9.70 shows the statistical significance of 99.99 % of the model which means that probability of failure of the model is 1 in 10,000. In addition, the randomization test shows confidence of ~99.9 % that the generated model is not random, and hence, it is chosen as the QSAR model. The plot of observed versus predicted activity (Table 4 and Fig. 4) provides an idea about how well the model was trained and how well it predicts the activity of the external test set.

From the plot, it can be seen model is able to predict the activity of training set quite well (all points are close to regression line) as well as external test setup to ~60 % (only 1 point is relatively apart from the regression line) providing confidence in predictive ability of the model. The developed MLR model reveals that the descriptor T_T_N_3 (i.e., any atom separated from nitrogen atom by three bonds in a molecule) plays most important role (~60 %) in determining anticonvulsant activity (Fig. 5), which mainly indicates the relationship with reference to the introduction of a substituent at 3-position on the pyrazole nucleus, or at 8- or 17-position on the pyridine ring. The second descriptor SK MostHydrophobicHydrophilicDistance contributed negatively (~40 %) that indicates that greater the distance between hydrophilic (e.g., $-NH_2$) and hydrophobic (e.g., $-C_6H_5$) groups in the molecule, the lesser will be its activity. Taking into consideration, both these descriptors, a pyrazolyl pyridine having, for example, 3-NH_2 and 8- or 17-C_6H_5, may be more promising anticonvulsant (Fig. 6). Also, importance of substituents at positions other than those present in the designed compounds verified the results of pharmacological screening that variety of substituent in the active compounds gave similar results, most probably due to the reason that present position of substituents was not important. Requirement of lesser distance between R_1 and R_2 further proves that smaller molecules show better activity as observed with the results of anticonvulsant screening.

Along with 2D QSAR analysis, the compounds were also subjected to 3D QSAR analysis by k-nearest neighbor molecular field analysis (KNN-MFA) in conjunction with stepwise (SW) forward–backward, genetic algorithm (GA), and simulated annealing (SA) variable selection methods using the software VLife MDS. The best model selected was having nearly the same observed and predicted activities of the compounds (Table 5, Fig. 7).

Selected descriptors:	S_442, S_164,E_272, E_442
Descriptor range:	S_442: −0.1376 to −0.1324, S_164: 30.0000 to 30.0000, E_272: −0.3004 to 0.8490, E_442: 5.2188 to 10.0000
k-nearest neighbor:	2
n:	14
Degree_of_freedom:	9
q^2:	0.7873
q^2_se:	0.1440
pred_r^2:	0.3835
pred_r^2se:	0.2898

The above KNN-MFA model obtained by simulated annealing variable selection method shows that electrostatic interactions (E_272 and E_442 are electrostatic field descriptors, former having a negative to positive range while later having a positive range) as well as steric interactions (S_442 and S_164 are steric field descriptors, former having a negative range while later having a positive range) play major role in determining biological activity. Negative range of electrostatic field descriptor indicates that negative electrostatic potential is favorable for increase in the activity, and hence, a more electronegative substituent group is preferred in that region, while positive range indicates that positive electrostatic potential is favorable for increase in the activity and hence a less electronegative substituent group is preferred in that region. A negative range of steric field descriptor indicates that negative steric potential is favorable for increase in the activity and hence less bulky substituent group is preferred in that region while positive range indicates that positive steric potential is favorable for increase in the activity and hence more bulky substituent group is preferred in that region.

Statistically SA-KNN-MFA model was comparatively better than the other two with respect to the internal ($q^2 = 0.78$) as well as the external (pred_$r^2 = 0.38$) model

Table 4 Observed and predicted values of the compounds **7–27** for the best model obtained through 2D QSAR

Compound code	−log (% inhibition)		
	Observed value	Predicted value	Residual value
7.	−1.965	−1.92355	−0.04145
8.	−1.965	−1.57528	−0.38972
9.	−1.98	−1.84207	−0.13793
10.	−1.974	−2.17589	0.201894
11.	−1.97	−2.02769	0.057691
12.	−1.928	−2.03513	0.107129
13.	−1.213	−1.31367	0.100665
14.	−1.937	−1.76902	−0.16798
15.	−1.947	−2.37278	0.425783
16.	−1.305	−1.79467	0.489673
17.	−1.414	−1.45282	0.038818
18.	−1.974	−1.80739	−0.16661
19.	−1.937	−2.08528	0.148277
20.	−1.983	−2.20621	0.223211
21.	−1.429	−2.20291	0.773908
22.	−1.098	−1.52125	0.423253
23.	−1.965	−1.71268	−0.25233
24.	−1.965	−1.71287	−0.25213
25.	−1.992	−1.95584	−0.03616
26.	−1.928	−1.96255	0.034553
27.	−1.238	−1.65765	0.419654

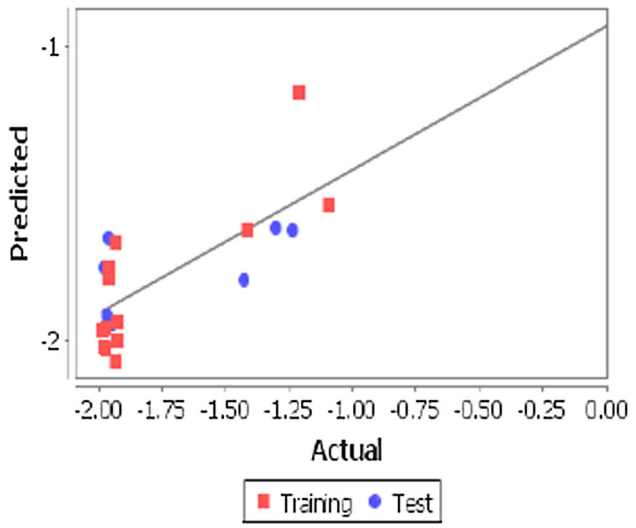

Fig. 4 Observed versus predicted anticonvulsant activity of test and training sets obtained through 2D QSAR

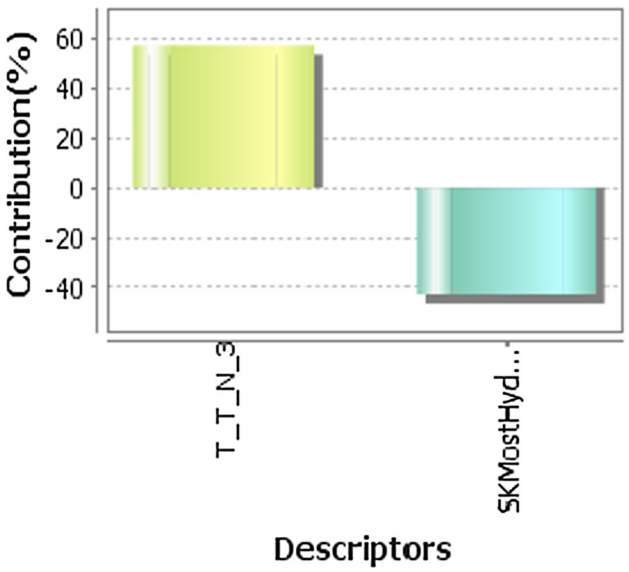

Fig. 5 Contribution plot of statistically significant model obtained through 2D QSAR

validation and correctly predicts activity ~78 and ~38 % for the training and test set, respectively. It uses 2 electrostatic and 2 steric field descriptors along with its 2 k nearest neighbor ($k = 2$) to evaluate the activity of new molecule. Plot of the KNN-MFA which shows the relative position and ranges of the corresponding important electrostatic/steric fields in the model provides the following guidelines for design of new molecule. The 3D plot

(Fig. 8) shows the electrostatic and steric fields important for interaction of molecules with space, i.e., with receptor, thereby affecting the pharmacologic response. As was observed with the pharmacological activity of present set of compounds, the ones having substituents with similar electronic character on both the pyridine rings were mostly fond to be inactive (e.g., **13**, **16**, **17,** and **27**) while compounds having substituents with different electronic character on either of the pyridine ring were active (e.g., **8**, **9**, **10**, **18**, and **19**). A more bulky substitution at S_442 that most of the inactive compounds had (e.g., comp. **16**, **17**, **21**, and **17**) did not favor the activity; as a more bulky substitution may block the entrance to the binding pocket of the receptor and if it is less bulky, it would permit the entrance. However, the results suggested, as with 2D QSAR analysis, a more bulky substitution at S_164, i.e., at 8- or 17-position of the parent molecule (Fig. 4) may be allowed for the better activity. Thus, modification of these fields according to the ranges obtained may result into more potent compounds.

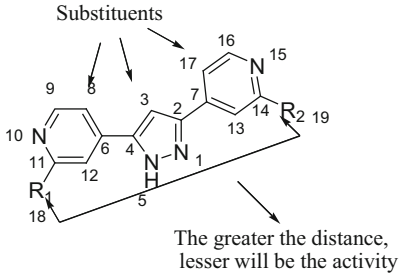

e.g. 3- NH_2 and 8-or 17-C_6H_5 may have good Anticonvulsant activity.

Fig. 6 Suggestions according to the result of 2D QSAR analysis for design of improved anticonvulsant drugs

Experimental

Chemistry

All the chemicals and solvents were purchased from Sigma-Aldrich and were used without further purification. Melting points were taken in open capillary tubes and are uncorrected. The progress of the reaction as well as purity of the compounds was confirmed by TLC using Merck silica gel 60 F_{254}-coated aluminum plates using chloroform–methanol (9:1) as solvent and detection by UV light. IR spectra were recorded on a Bruker-alpha FTIR spectrometer (ν max in cm^{-1}). ^{1}H-NMR and ^{13}C-NMR spectra were recorded on Bruker NMR spectrometers (400 MHz

Table 5 Observed and predicted values of the compounds according to the best model obtained through 3D QSAR

Compound code	−log (% inhibition)		
	Observed value	Predicted value	Residual value
7.	−1.965	−1.97891	0.01391
8.	−1.965	−1.97677	0.011768
9.	−1.98	−1.9688	−0.0112
10.	−1.974	−1.9765	0.002501
11.	−1.97	−1.77761	−0.19239
12.	−1.928	−1.6895	−0.2385
13.	−1.213	−1.38682	0.173818
14.	−1.937	−1.94002	0.003021
15.	−1.947	−1.937	−0.01
16.	−1.305	−1.57614	0.271137
17.	−1.414	−1.513	0.099
18.	−1.974	−1.6865	−0.2875
19.	−1.937	−1.94274	0.005741
20.	−1.983	−1.96148	−0.02152
21.	−1.429	−1.96037	0.531367
22.	−1.098	−1.38351	0.28551
23.	−1.965	−1.95859	−0.00641
24.	−1.965	−1.96482	−0.00018
25.	−1.992	−1.92806	−0.06394
26.	−1.928	−1.99187	0.063871
27.	−1.238	−1.57028	0.332281

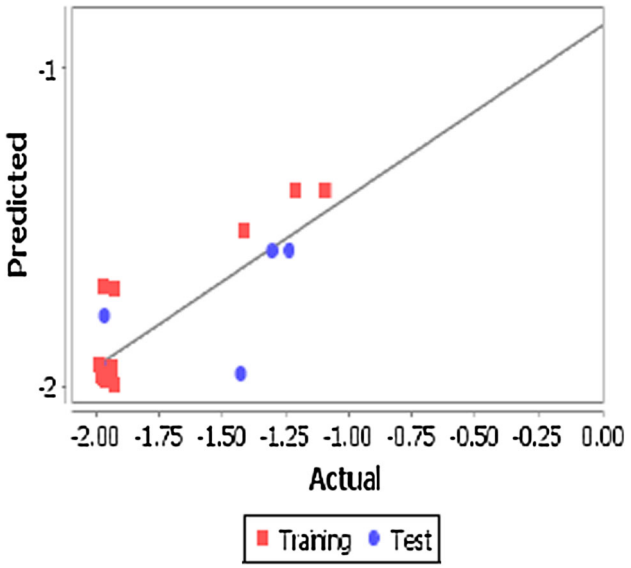

Fig. 7 Observed versus predicted anticonvulsant activity of test and training sets obtained through 3D QSAR

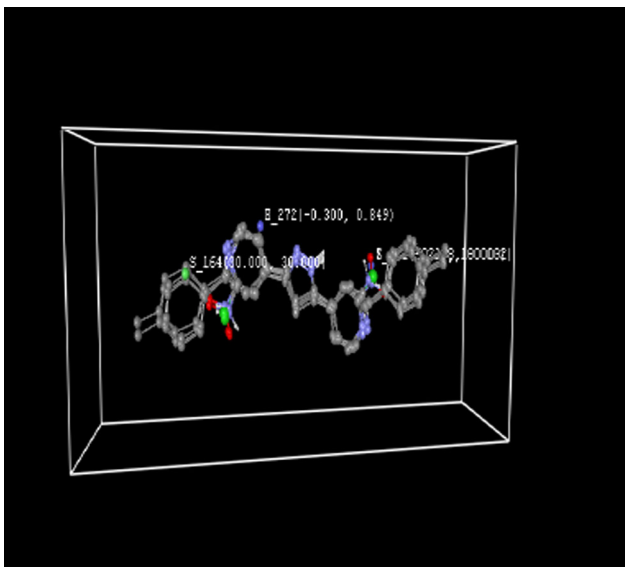

Fig. 8 3D plot of statistically significant model obtained through KNN-MFA

for ^{1}H-NMR, and 100 and 125 MHz for ^{13}C-NMR) using TMS as the internal standard. MS spectra were recorded on Water's TOF Micro mass LC–MS spectrophotometer. Microanalysis was performed on a PerkinElmer-240 CHN elemental analyzer.

*General procedure for the synthesis of title compounds (**7–27**)*

Appropriate acetone (intermediates **1a–6a**; 2 m mol) was dissolved in 5 ml of dry toluene in a 100-ml RBF with a septum, and the solution was cooled to 0 °C under nitrogen. LiHMDS (2.1 ml, 1.0 M in THF, 2.1 m mol) was added quickly via syringe with stirring. After 1 min., substituted isonicotinoyl chloride hydrochloride (intermediates **1b–6b**; 1 m mol) was added in one portion with stirring. The flask was then removed from the ice bath and allowed to stand for 1 min, and then 2 ml of AcOH was added with stirring. EtOH (10 ml) and THF (5 ml) were added to form a homogenous mixture, and then hydrazine hydrate (2 ml, 1.1 g, and 34.43 m mol) was added. The mixture was allowed to auto reflux and was held at that temperature for 5 min or until the reaction completes. The resulting solution was added to 1.0 M NaOH solution and extracted with EtOAc. The organic fraction was then washed with brine, dried over Na_2SO_4, and evaporated under reduced pressure. The resulting residue was recrystallized from 2-propanol/water to afford the product (compounds **7–27**).

4-(3-(Pyridin-4-yl)-1H-pyrazol-5-yl)pyridine (**7**) Yellow–brown powder; Yield: 65 %; m.p.: 236–238 °C; Rf: 0.71; FT-IR υ_{max} (ATR cm^{-1}): 3388 (2°N–H str. in pyrazole), 3036 (aromatic C–H str.), 1650 (C=N str.), 1407, 1486, 1538 (C=C str. aromatic), 1239 (C–N str.), 1128 (N–H bend.), ^{1}H NMR (DMSO-d_6, 400 MHz,): δ = 10.28 (s, 1H, NH), 8.61–8.64 (d, 4H, Ar–H), 7.54–7.57 (d, 4H, Ar–H), 7.05 (s, 1H, CH). ^{13}C NMR (100 MHz, common NMR solvents) δ 150.7 (2C, C–Ar), 149.6 (2C, C–Ar), 147.5 (C_5), 146.8 (C_3), 134. 4 (C–Ar), 132.8 (C–Ar), 120.7 (2C, C–Ar), 119.8 (2C, C–Ar), 102.1 (C_4). LCMS *m/z* [M]$^{+}$ 222.09. Anal. Calcd. for $C_{13}H_{10}N_4$ (222.25): C, 70.26; H, 4.54; N, 25.21. Found: C, 70.16; H, 4.51; N, 25.11.

2-Nitro-4-(3-(pyridin-4-yl)-1H-pyrazol-5-yl)pyridine (**8**) Yellow powder; Yield: 63 %; m.p.: 220–224 °C; R_f: 0.62; FT-IR υ_{max} (ATR cm^{-1}): 3174 (2°N–H str. in pyrazole), 3036 (aromatic C–H str.), 1650 (C=N str.), 1407,1486,1538 (C=C str. aromatic), 1239 (C–N str.), 1127 (N–H bend.), 1630, 1407 (N=O str.). ^{1}H NMR (DMSO-d_6, 400 MHz,): δ = 10.13 (s, 1H, NH), 8.82–8.83 (d, 1H, Ar–H), 8.61 (s, 1H, Ar–H), 8.53–8.55 (d, 2H, Ar–H), 8.21–8.23 (d, 1H, Ar–H), 7.50–7.51 (d, 2H, Ar–H), 6.87 (s, 1H, CH). ^{13}C NMR (125 MHz, common NMR solvents) δ 159.1 (C–Ar), 150.1 (2C, C–Ar), 149.85 (C–Ar), 147.45 (C_5), 146.18 (C_3), 134.44 (C–Ar), 134.24 (C–Ar), 123.99 (C–Ar), 119.80 (2C, C–Ar), 117.69 (C–Ar), 103.52 (C_4). LCMS *m/z* [M]$^{+}$ 267.23. Anal. Calcd. for $C_{13}H_9N_5O_2$ (267.24): C, 58.43; H, 3.39; N, 26.21. Found: C, 58.13; H, 3.29; N, 26.21.

4-(3-(Pyridin-4-yl)-1H-pyrazol-5-yl)pyridin-2-amine (**9**) Pale yellow powder; Yield: 68 %; m.p.: 310–312 °C; R_f: 0.6; FT-IR υ_{max} (ATR cm^{-1}): 3405, 3382 (1°NH_2 str.), 3038 (aromatic C–H str.), 1588 (C=N str.), 1415, 1492, 1512

(C=C str. aromatic), 1588 (C–N str.). ^{1}H NMR (DMSO-d_6, 400 MHz,): δ = 10.31 (s, 1H, NH), 8.64–8.66 (d, 2H, Ar–H), 8.19–8.21 (d, 1H, Ar–H), 7.57–7.58 (d, 2H, Ar–H), 7.08 (s, 1H, CH), 6.94–6.95 (d, 2H, Ar–H), 1.49 (s, 2H, NH_2). ^{13}C NMR (125 MHz, common NMR solvents) δ 159.45 (C–Ar), 150.58 (2C, C–Ar), 149.15 (C–Ar), 147.45 (C_5), 146.24 (C_3), 136.11 (C–Ar), 134.24 (C–Ar), 119.80 (2C, C–Ar), 108.69 (C–Ar), 106.78 (C–Ar), 103.42 (C_4). LCMS *m/z* $[M]^+$ 237.10. Anal. Calcd. for $C_{13}H_{11}N_5$ (237.26): C, 65.81; H, 4.67; N, 29.52. Found: C, 64.13; H, 4.29; N, 29.21.

2-Chloro-4-(3-(pyridin-4-yl)-1H-pyrazol-5-yl)pyridine (**10**) Pale white powder; Yield: 58 %; m.p.: 319–321 °C; R_f: 0.7; FT-IR υ_{max} (ATR cm^{-1}): 3382 (2°N–H str. in pyrazole), 3039 (aromatic C–H str.), 1590 (C=N str.), 1417, 1476, 1511 (C=C str. aromatic), 1239 (C–N str.).^{1}H NMR (DMSO-d_6, 400 MHz,): δ = 10.06 (s, 1H, NH), 8.52–8.54 (d, 1H, Ar–H), 8.43–8.44 (d, 2H, Ar–H), 7.79 (s, 1H, Ar–H), 7.62–7.64 (d, 1H, Ar–H), 7.39–7.41 (d, 2H, Ar–H), 7.26 (s, 1H, CH). 13C NMR (125 MHz, common NMR solvents) δ 150.93 (C–Ar), 150.58 (2C, C–Ar), 149.12 (C–Ar), 147.65 (C5), 146.15 (C3), 134.14 (C–Ar), 134.29 (C–Ar), 121.45 (C–Ar), 120.28 (C–Ar), 119.80 (2C, C–Ar), 103.42 (C4). LCMS *m/z* $[M]^+$ 256.21. Anal. Calcd. for $C_{13}H_9ClN_4$ (256.69): C, 60.83; H, 3.53; Cl, 13.81; N, 21.83. Found: C, 60.86; H, 3.43; N, 21.66.

2-Phenyl-4-(3-(pyridin-4-yl)-1H-pyrazol-5-yl)pyridine (**11**) Pale brown powder; Yield: 62 %; m.p.: 330–332 °C; R_f: 0.75; FT-IR υ_{max} (ATR cm^{-1}): 3374 (2°N–H str. in pyrazole), 3030 (aromatic C–H str.), 1590 (C=N str.), 1521, 1602, 1708 (C=C str. aromatic), 1345 (C–N str.). ^{1}H NMR (DMSO-d_6, 400 MHz,): δ = 10.18 (s, 1H, NH), 8.46–8.49 (d, 2H, Ar–H), 7.85 (s, 1H, Ar–H), 7.74–7.76 (m, 2H, Ar–H), 7.50 (s, 1H, CH), 7.41–7.43 (m, 3H, Ar–H), 7.11–7.23 (m, 3H, Ar–H). ^{13}C NMR (125 MHz, common NMR solvents) δ 159.38 (C–Ar), 150.48 (C–Ar), 148.03 (C–Ar), 147.35 (C5), 146.18 (C3), 138.49 (C–Ar), 137.31 (C–Ar), 134.24 (C–Ar), 130.08 (C–Ar), 128.96 (2 C, C–Ar), 127.92 (2C, C–Ar), 120.42 (C–Ar), 119.68 (2C, C–Ar), 117.38 (C–Ar), 103.22 (C4). LCMS *m/z* $[M]^+$ 298.12. Anal. Calcd. for $C_{19}H_{14}N_4$ (298.34): C, 76.49; H, 4.73; N, 18.78. Found: C, 76.49; H, 4.80; N, 18.68.

4-(3-(Pyridin-4-yl)-1H-pyrazol-5-yl)-2-p-tolylpyridine (**12**) Pale yellow powder; Yield: 59 %; m.p.: 260–262 °C; R_f: 0.78; FT-IR υ_{max} (ATR cm^{-1}): 3374 (2°N–H str. in pyrazole), 3030 (aromatic C–H str.), 1708 (C=N str.), 1521, 1538, 1602 (C=C str. aromatic), 1345 (C–N str.). ^{1}H NMR (DMSO-d_6, 400 MHz,): δ = 10.24 (s, 1H, NH), 8.53–8.55 (d, 3H, Ar–H), 7.91 (s, 1H, Ar–H), 7.76–7.77 (m, 2H, Ar–H), 7.51 (s, 1H, CH), 7.47–7.50 (m, 2H, Ar–H), 7.14–7.23 (m, 3H, Ar–H), 2.20 (s, 3H, CH_3). ^{13}C NMR (125 MHz, common NMR solvents) δ 159.54 (C–Ar), 150.58 (2C, C–Ar), 148.06 (C–Ar), 147.45 (C5), 146.18 (C3), 141.24 (C–Ar), 137.25 (C–Ar), 136.72 (C–Ar), 134.22 (C–Ar), 130.25 (2C, C–Ar), 128.21 (2C, C–Ar), 120.50 (C–Ar), 119.82 (2C, C–Ar), 117.40 (C–Ar), 103.51 (C4), 21.11 (CH3). LCMS *m/z* $[M]^+$ 312.13. Anal. Calcd. for $C_{20}H_{16}N_4$ (312.37): C, 76.90; H, 5.16; N, 17.94. Found: C, 76.88; H, 5.26; N, 17.82.

2-Nitro-4-(3-(2-nitropyridin-4-yl)-1H-pyrazol-5-yl)pyridine (**13**) Bright yellow crystals; Yield: 68 %; m.p.: 320–322 °C; R_f: 0.56; FT-IR υ_{max} (ATR cm^{-1}): 3176 (2°N–H str. in pyrazole), 3106 (aromatic C–H str.), 1615 (C=N str.), 1597, 1343 (N=O str.), 1343 (C–N str.), 1211 (N–H bend.). ^{1}H NMR (DMSO-d_6, 400 MHz,): δ = 10.11 (s, 1H, NH), 8.70–8.71 (d, 2H, Ar–H), 8.54 (s, 2H, Ar–H), 8.06–8.13 (m, 2H, Ar–H), 7.35 (s, 1H, CH). ^{13}C NMR (125 MHz, common NMR solvents) δ 159.09 (C–Ar), 157.94 (C–Ar), 150.02 (C–Ar), 149.75 (C–Ar), 147.86 (C5), 146.16 (C3), 135.35 (C–Ar), 134.42 (C–Ar), 125.15 (C–Ar), 123.96 (C–Ar), 118.89 (C–Ar), 117.65 (C–Ar), 103.50 (C4). LCMS *m/z* $[M]^+$ 312.48. Anal. Calcd. for $C_{13}H_8N_6O_4$ (312.24): C, 50.01; H, 2.58; N, 26.92. Found: C, 50.11; H, 2.52; N, 26.86.

4-(3-(2-Aminopyridin-4-yl)-1H-pyrazol-5-yl)pyridin-2-amine (**14**) Pale yellow powder; Yield: 62 %; m.p.: 350–352 °C; R_f: 0.62; FT-IR υ_{max} (ATR cm^{-1}): 3405, 3382 (1°NH_2 aromatic), 3038 (aromatic C–H str.), 1660 (C=N str.), 1415, 1482, 1511 (C=C str. aromatic), 1242 (C–N str.).^{1}H NMR (DMSO-d_6, 400 MHz,): δ = 10.11 (s, 1H, NH), 8.70–8.71 (d, 2H, Ar–H), 8.54 (s, 2H, Ar–H), 8.06–8.13 (m, 2H, Ar–H), 7.35 (s, 1H, CH). ^{13}C NMR (125 MHz, common NMR solvents) δ 161.05 (C–Ar), 159.45 (C–Ar), 149.73 (C–Ar), 149.15 (C–Ar), 147.88 (C5), 146.48 (C3), 139.16 (C–Ar), 135.83 (C–Ar),110.48 (C–Ar), 109.02 (C–Ar), 108.69 (C–Ar), 106.98 (C–Ar), 103.52 (C4). LCMS *m/z* $[M]^+$ 252.11. Anal. Calcd. for $C_{13}H_{12}N_6$ (252.27): C, 61.89; H, 4.79; N, 33.31. Found: C, 61.86; H, 4.68; N, 33.33.

2-Chloro-4-(3-(2-chloropyridin-4-yl)-1H-pyrazol-5-yl)pyridine (**15**) Pale white powder; Yield: 58 %; m.p.: 380–281 °C; R_f: 0.65; FT-IR υ_{max} (ATR cm^{-1}): 3242 (2°N–H str. in pyrazole), 2918 (aromatic C–H str.), 1663 (C=N str.), 1433, 1475, 1576 (C=C str. aromatic), 1238 (C–N str.), 705 (C–Cl). ^{1}H NMR (DMSO-d_6, 400 MHz,): δ = 10.62 (s, 1H, NH), 8.52–8.54 (d, 2H, Ar–H), 7.78 (s, 2H, Ar–H), 7.61–7.66 (m, 2H, Ar–H), 6.87 (s, 1H, CH). ^{13}C NMR (125 MHz, common NMR solvents) δ 153.19 (C–Ar), 150.93 (C–Ar), 150.72, 149.42 (C–Ar), 147.88 (C5), 146.14 (C3), 136.68 (C–Ar), 134.29 (C–Ar), 121.42 (C–Ar), 120.45 (2C, C–Ar), 118.72 (C–Ar), 103.46 (C4).

LCMS *m/z* $[M]^+$ 290.01. Anal. Calcd. for $C_{13}H_8C_{l2}N_4$ (291.14): C, 53.63; H, 2.77; N, 19.24. Found: C, 53.64; H, 2.74; Cl, 24.38; N, 19.18.

2-Phenyl-4-(3-(2-phenylpyridin-4-yl)-1H-pyrazol-5-yl)pyridine (**16**) Yellowish-white powder; Yield: 70 %; m.p.: 293–297 °C; R_f: 0.72; FT-IR υ_{max} (ATR cm^{-1}): 3310 (2°N–H str. in pyrazole), 3047 (aromatic C–H str.), 1591 (C=N str.), 1409, 1494, 1519 (C=C str. aromatic), 1269 (C–N str.). ^{1}H NMR (DMSO-d_6, 400 MHz,): $\delta = 10.27$ (s, 1H, NH), 8.56–8.55 (d, 2H, Ar–H), 7.93 (m, 4H, Ar–H), 7.78–7.81 (m, 2H, Ar–H), 7.51 (s, 1H, CH), 7.16–7.30 (m, 6H, Ar–H). ^{13}C NMR (125 MHz, common NMR solvents) δ 161.00 (C–Ar), 159.54 (C–Ar), 148.06 (2C, C–Ar), 147.88 (C5), 146.18 (C3), 138.59 (2C, C–Ar), 137.84 (C–Ar), 137.35 (C–Ar), 130.08 (2C, C–Ar), 128.96 (4C, C–Ar), 127.96 (4C, C–Ar), 120.93 (C–Ar), 120.52 (C–Ar), 117.82 (C–Ar), 117.42 (C–Ar), 103.52 (C4). LCMS *m/z* $[M]^+$ 374.15. Anal. Calcd. for $C_{25}H_{18}N_4$ (374.44): C, 80.19; H, 4.85; N, 14.96. Found: C, 80.16; H, 4.78; N, 14.88.

2-p-Tolyl-4-(3-(2-p-tolylpyridine-4-yl)-1H-pyrazol-5-yl)pyridine (**17**) Pale yellow brown powder; Yield: 60 %; m.p.: 343–346 °C; R_f: 0.71; FT-IR υ_{max} (ATR cm^{-1}): 3310 (2°N–H str. in pyrazole), 3047 (aromatic C–H str.), 1591 (C=N str.), 1409,1477, 1575 (C=C str. aromatic), 1241 (C–N str.). ^{1}H NMR (DMSO-d_6, 400 MHz,): $\delta = 10.33$ (s, 1H, NH), 8.62–8.64 (d, 2H, Ar–H), 7.92–7.94 (d, 2H, Ar–H), 7.75–7.78 (m, 4H, Ar–H), 7.42 (s, 1H, CH), 7.16–7.33 (m, 6H, Ar–H), 2.23 (s, 6H, CH_3). ^{13}C NMR (125 MHz, common NMR solvents) δ 161.00 (C–Ar), 159.54 (C–Ar), 148.06 (C–Ar), 147.88 (C5), 146.18 (C3), 141.24 (C–Ar), 137.84 (C–Ar), 137.35 (C–Ar), 136.72 (2C, C–Ar), 130.27 (4C, C–Ar), 128.23 (4C, C–Ar), 120.93 (C–Ar), 120.52 (C–Ar), 117.82 (C–Ar), 117.42 (C–Ar), 103.52 (C4), 21.13 (2C, CH3). LCMS *m/z* $[M]^+$ 402.18. Anal. Calcd. for $C_{27}H_{22}N_4$ (402.49): C, 80.57; H, 5.51; N, 13.92. Found:C, 80.47; H, 5.70; N, 13.88.

4-(3-(2-Chloropyridin-4-yl)-1H-pyrazol-5-yl)-2-nitropyridine (**18**) Pale yellow powder; Yield: 68 %; m.p.: 294–296 °C; R_f: 0.68; FT-IR υ_{max} (ATR cm^{-1}): 3261 (2°N–H str. in pyrazole), 2919 (aromatic C–H str.), 1576 (C=N str.), 1371, 1475, 1539 (C=C str. aromatic), 1586, 1475 (N=O str.), 1378 (C–N str.), 694 (C–Cl). ^{1}H NMR (DMSO-d_6, 400 MHz,): $\delta = 9.90$ (s, 1H, NH), 8.80–8.82 (d, 1H, Ar–H), 8.61 (d, 1H, Ar–H), 8.26 (s, 1H, CH), 8.08–8.09 (d, 1H, Ar–H), 7.87 (s, 1H, Ar–H), 7.79–7.81 (d, 1H, Ar–H), 6.86 (s, 1H, Ar–H). ^{13}C NMR (125 MHz, common NMR solvents) δ 159.09 (C–Ar), 153.19 (C–Ar), 150.75 (C–Ar), 149.85 (C–Ar), 147.88 (C5), 146.18 (C3), 136.70 (C–Ar), 134.44 (C–Ar), 123.99 (C–Ar), 120.45 (C–Ar), 118.72 (C–Ar), 117.69 (C–Ar), 103.52 (C4). LCMS *m/z* $[M]^+$ 301.03. Anal. Calcd. for $C_{13}H_8ClN_5O_2$ (301.69): C, 51.76; H, 2.67; N, 23.21. Found: C, 51.66; H, 2.57; N, 23.18.

4-(3-(2-Chloropyridin-4-yl)-1H-pyrazol-5-yl)pyridin-2-amine (**19**) Yellow powder; Yield: 58 %; m.p.: 312–314 °C; R_f: 0.62; FT-IR υ_{max} (ATR cm^{-1}): 3405, 3382 (1°N–H str.), 3039 (aromatic C–H str.), 1588 (C=N str.), 1415, 1492, 1511 (C=C str. aromatic), 1588 (C–N str.),666 (C–Cl). ^{1}H NMR (DMSO-d_6, 400 MHz,): $\delta = 9.85$ (s, 1H, NH), 8.75 (d, 1H, Ar–H), 8.14 (d, 1H, Ar–H), 7.75 (d, 1H, Ar–H), 7.70 (s, 1H, Ar–H), 6.98 (s, 1H, CH), 6.85–6.86 (d, 2H, Ar–H), 1.43 (s, 2H, NH_2). ^{13}C NMR (125 MHz, common NMR solvents) δ 157.08 (C–Ar), 153.17 (C–Ar), 150.75 (C–Ar), 147.85 (C5), 147.67 (C–Ar), 136.70 (C–Ar), 135.74 (C–Ar), 134.30 (C3), 120.43 (C–Ar), 118.69 (C–Ar), 113.77 (C–Ar), 113.39 (C–Ar), 101.30 (C4). LCMS *m/z* $[M]^+$ 271.16. Anal. Calcd. for $C_{13}H_{10}ClN_5$ (271.7): C, 57.47; H, 3.71; N, 25.78. Found: C, 57.44; H, 3.76; N, 25.74.

4-(3-(2-Chloropyridin-4-yl)-1H-pyrazol-5-yl)-2-phenylpyridine (**20**) Pale white powder; Yield: 57 %; m.p.: 245–247 °C; R_f: 0.69; FT-IR υ_{max} (ATR cm^{-1}): 3392 (2°N–H str. in pyrazole), 3047 (aromatic C–H str.), 1590 (C=N str.), 1387, 1414, 1493 (C=C str. aromatic), 1242 (C–N str.). ^{1}H NMR (DMSO-d_6, 400 MHz,): $\delta = 10.23$ (s, 1H, NH), 8.61–8.63 (d, 1H, Ar–H), 8.53–8.54 (d, 1H, Ar–H), 7.77–7.90 (m, 5H, Ar–H), 7.45 (s, 1H, CH), 7.17–7.36 (m, 4H, Ar–H). ^{13}C NMR (125 MHz, common NMR solvents) δ 159.54 (C–Ar), 153.19 (C–Ar), 150.75 (C–Ar), 148.06 (C–Ar), 147.88 (C5), 146.18 (C3), 138.59 (C–Ar), 137.35 (C–Ar), 136.70 (C–Ar), 130.08 (C–Ar), 128.92 (2C, C–Ar), 127.86 (2C, C–Ar), 120.52 (C–Ar), 120.44 (C–Ar), 118.72 (C–Ar), 117.42 (C–Ar), 103.48 (C4). LCMS *m/z* $[M]^+$ 332.08. Anal. Calcd. for $C_{19}H_{13}ClN_4$ (332.79): C, 68.57; H, 3.94; N, 16.84. Found: C, 68.59; H, 3.98; N, 16.84.

4-(3-(2-Chloropyridin-4-yl)-1H-pyrazol-5-yl)-2-p-tolylpyridine (**21**) Pale yellow powder; Yield: 65 %; m.p.: 276–278 °C; R_f: 0.64; FT-IR υ_{max} (ATR cm^{-1}): 3391 (2°N–H str. in pyrazole), 3047 (aromatic C–H str.), 1590 (C=N str.), 1240 (C–N str.). ^{1}H NMR (DMSO-d_6, 400 MHz,): $\delta = 10.20$ (s, 1H, NH), 8.61 (d, 1H, Ar–H), 8.50 (d, 1H, Ar–H), 7.72–7.87 (m, 5H, Ar–H), 7.42 (s, 1H, CH), 7.11–7.20 (m, 3H, Ar–H), 2.16 (s, 3H, CH_3). ^{13}C NMR (125 MHz, common NMR solvents) δ 159.48 (C–Ar), 153.19 (C–Ar), 150.65 (C–Ar), 148.06 (C–Ar), 147.82 (C_5), 146.18 (C_3), 141.24 (C–Ar), 137.35 (C–Ar), 136.70 (C–Ar), 136.70 (C–Ar), 130.24 (C–Ar), 130.27 (C–Ar), 128.19 (C–Ar), 103.39 (C_4), 21.11 (CH_3). LCMS *m/z* $[M]^+$ 346.09. Anal. Calcd. for $C_{20}H_{15}ClN_4$ (346.81): C, 69.26; H, 4.36; N, 16.15. Found: C, 69.16; H, 4.28; N, 16.21.

4-(5-(2-Nitropyridin-4-yl)-1H-pyrazol-3-yl)pyridin-2-amine (**22**) Orange-Yellow powder; Yield: 58 %; m.p.: 324–326 °C; R_f: 0.55; FT-IR υ_{max} (ATR cm^{-1}): 3308, 3383 (1° N–H str. in aromatic amines) 3177 (2°N–H str. in pyrazole), 3039 (aromatic C–H str.), 1650 (C=N str.), 1599, 1411 (N=O str.) 1491, 1509, 1336 (C=C str. aromatic), 1242 (C–N str.),1212 (N–H bend). ^{1}H NMR (DMSO-d_6, 400 MHz,): δ = 10.28 (s, 1H, NH), 8.89–8.90 (d, 1H, Ar–H), 8.74 (s, 1H, Ar–H), 8.19–8.27 (m, 2H, Ar–H), 7.55 (s, 1H, CH), 6.95–7.01 (m, 2H, Ar–H), 1.51 (s, 2H, NH_2). ^{13}C NMR (125 MHz, common NMR solvents) δ 161.05 (C–Ar), 159.09 (C–Ar), 149.85 (C–Ar), 149.73 (C–Ar), 147.88 (C5), 146.18 (C3), 139.16 (C–Ar), 134.44 (C–Ar), 123.99 (C–Ar), 117.69 (C–Ar), 110.48 (C–Ar), 109.02 (C–Ar), 103.52 (C4). LCMS *m/z* $[M]^+$ 282.08. Anal. Calcd. for $C_{13}H_{10}N_6O_2$ (282.26): C, 55.32; H, 3.57; N, 29.77. Found: C, 55.22; H, 3.69; N, 29.58.

2-Nitro-4-(3-(2-phenylpyridin-4-yl)-1H-pyrazol-5-yl)pyridine (**23**) Yellow powder; Yield: 62 %; m.p.: 352–354 °C; R_f: 0.63; FT-IR υ_{max} (ATR cm^{-1}): 3106 (2°N–H str. in pyrazole), 3062 (aromatic C–H str.), 1612 (C=N str.), 1344 (C–N str.),1586, 1344 (N=O str.). ^{1}H NMR (DMSO-d_6, 400 MHz,): δ = 10.30 (s, 1H, NH), 8.85–8.87 (d, 1H, Ar–H), 8.71 (s, 1H, Ar–H), 8.60–8.62 (m, 1H, Ar–H), 8.21–8.23 (d, 1H, Ar–H), 7.98–7.99 (s, 1H, Ar–H), 7.87–7.89 (d, 2H, Ar–H), 7.59 (s, 1H, CH), 7.23–7.35 (m, 4H, Ar–H). ^{13}C NMR (125 MHz, common NMR solvents) δ 161.00 (C–Ar), 159.09 (C–Ar), 149.85 (C–Ar), 148.04 (C–Ar), 147.88 (C5), 146.18 (C3), 138.59 (C–Ar), 137.84 (C–Ar), 134.35 (C–Ar), 130.08 (C–Ar), 128.96 (2C, C–Ar), 127.96 (2C, C–Ar), 122.99 (C–Ar), 120.93 (C–Ar), 117.81 (C–Ar), 117.69 (C–Ar), 103.50 (C4). LCMS *m/z* $[M]^+$ 343.34. Anal. Calcd. for $C_{19}H_{13}N_5O_2$ (343.34): C, 66.47; H, 3.82; N, 20.40. Found: C, 66.45; H, 3.68; N, 20.20.

2-Nitro-4-(3-(2-p-tolylpyridine-4-yl)-1H-pyrazol-5-yl)pyridine (**24**) Pale yellow powder; Yield: 68 %; m.p.: 344–345 °C; R_f: 0.6; FT-IR υ_{max} (ATR cm^{-1}): 3106 (2°N–H str. in pyrazole), 3047 (aromatic C–H str.), 2872 (aliphatic C–H str.) 1597 (C=N str.), 1597, 1343 (N=O str.), 1270 (C–N str.), 1210 (N–H bend). ^{1}H NMR (DMSO-d_6, 400 MHz,): δ = 10.26 (s, 1H, NH), 8.82–8.83 (d, 1H, Ar–H), 8.68 (s, 1H, Ar–H), 8.56 (d, 1H, Ar–H), 8.18–8.20 (d, 1H, Ar–H), 7.94 (s, 1H, Ar–H), 7.79–7.81 (d, 2H, Ar–H), 7.56 (s, 1H, CH), 7.16–7.31 (m, 3H, Ar–H), 2.23 (s, 3H, CH_3). ^{13}C NMR (125 MHz, common NMR solvents) δ 161.00 (C–Ar), 159.09 (C–Ar), 149.85 (C–Ar), 148.04 (C–Ar), 147.88 (C5), 146.18 (C3), 141.24 (C–Ar), 137.84 (C–Ar), 136.72 (C–Ar), 134.44 (C–Ar), 130.27 (2C, C–Ar), 128.23 (2C, C–Ar), 124.09 (C–Ar), 121.03 (C–Ar), 117.82 (C–Ar), 117.66 (C–Ar), 102.99 (C4), 21.13 (CH3). LCMS *m/z* $[M]^+$ 357.12. Anal. Calcd. for $C_{20}H_{15}N_5O_2$ (357.37): C, 67.22; H, 4.23; N, 19.60. Found: C, 67.18; H, 4.25; N, 19.54.

4-(3-(2-Phenylpyridin-4-yl)-1H-pyrazol-5-yl)pyridin-2-amine (**25**) Yellow–brown powder; Yield: 61 %; m.p.: 352–355 °C; R_f: 0.74; FT-IR υ_{max} (ATR cm^{-1}): 3405, 3382 (1°N–H str. aromatic), 3040 (aromatic C–H str.), 1660 (C=N str.), 1415, 1466, 1513 (C=C str. aromatic), 1242 (C–N str.). ^{1}H NMR (DMSO-d_6, 400 MHz,): δ = 10.33 (s, 1H, NH), 8.63 (d, 1H, Ar–H), 8.17–8.19 (d, 1H, Ar–H), 8.00 (s, 1H, Ar–H), 7.89–7.91 (d, 2H, Ar–H), 7.50 (s, 1H, CH), 7.25–7.37 (m, 4H, Ar–H), 6.92–6.93 (m, 2H, Ar–H), 1.54 (s, 2H, NH_2). ^{13}C NMR (125 MHz, common NMR solvents) δ 159.48 (C–Ar), 159.25 (C–Ar), 149.15 (C–Ar), 147.04 (C–Ar), 147.98 (C_5), 146.15 (C_3), 138.55 (C–Ar), 137.82 (C–Ar), 135.78 (C–Ar), 130.05 (C–Ar), 128.92 (2C, C–Ar), 127.88 (2C, C–Ar), 120.94 (C–Ar), 117.72 (C–Ar), 108.69 (C–Ar), 106.98 (C–Ar), 103.45 (C_4). LCMS *m/z* $[M]^+$ 313.13. Anal. Calcd. for $C_{20}H_{17}N_5$ (327.38): C, 73.37; H, 5.23; N, 21.39. Found: C, 73.68; H, 5.82; N, 21.38.

4-(3-(2-p-tolylpyridine-4-yl)-1H-pyrazol-5-yl)pyridin-2-amine (**26**) Pale yellow powder; Yield: 63 %; m.p.: 286–287 °C; R_f: 0.64; FT-IR υ_{max} (ATR cm^{-1}): 3406, 3383 (1° N–H str. aromatic), 3178 (C–H str. aliphatic) 3083 (2°N–H str. in pyrazole), 3041 (aromatic C–H str.), 1589 (C=N str.), 1415, 1492, 1551 (C=C str. aromatic), 1242 (C–N str.). ^{1}H NMR (DMSO-d_6, 400 MHz,): δ = 10.24 (s, 1H, NH), 8.54 (d, 1H, Ar–H), 8.08–8.10 (d, 1H, Ar–H), 7.91 (s, 1H, Ar–H), 7.75–7.77 (d, 2H, Ar–H), 7.41 (s, 1H, CH), 7.27 (d, 1H, Ar–H), 7.13–7.14 (d, 2H, Ar–H), 6.83 (s, 2H, Ar–H), 2.18 (s, 3H, CH_3), 1.46 (s, 2H, NH_2). 13C NMR (125 MHz, common NMR solvents) δ 161.00 (C–Ar), 159.41 (C–Ar), 149.11 (C–Ar), 148.02 (C–Ar), 147.85 (C5), 146.16 (C3), 141.14 (C–Ar), 137.77 (C–Ar), 136.70 (C–Ar), 135.78 (C–Ar), 130.22 (2C, C–Ar), 128.23 (2C, C–Ar), 120.83 (C–Ar), 117.79 (C–Ar), 108.58 (C–Ar), 106.87 (C–Ar), 102.82 (C4), 21.13 (CH3). LCMS *m/z* $[M]^+$ 327.14. Anal. Calcd. for $C_{20}H_{17}N_5$ (327.38): C, 73.37; H, 5.23; N, 21.39. Found: C, 73.32; H, 5.32; N, 21.43.

2-Phenyl-4-(3-(2-p-tolylpyridine-4-yl)-1H-pyrazol-5-yl)pyridine (**27**) Pale brown powder; Yield: 57 %; m.p.: 347–349 °C; R_f: 0.58; FT-IR υ_{max} (ATR cm^{-1}): 3389 (2°N–H str. in pyrazole), 3178 (C–H str. aliphatic) 3047 (aromatic C–H str.), 1660 (C=N str.), 1408, 1463, 1538 (C=C str. aromatic), 1269 (C–N str.). ^{1}H NMR (DMSO-d_6, 400 MHz,): δ = 10.37 (s, 1H, NH), 8.65 (d, 2H, Ar–H), 8.01 (s, 2H, Ar–H), 7.84–7.89 (m, 4H, Ar–H), 7.60 (s, 1H, CH), 7.21–7.38 (d, 7H, Ar–H), 2.28 (s, 3H, CH_3). 13C NMR (125 MHz, common NMR solvents) δ 161.05 (C–Ar), 159.54 (C–Ar), 148.04 (C–Ar), 148.04 (C–Ar), 147.68

Table 6 Unicolumn statistics of selected training and test sets for 2D QSAR model development of compound for antiepileptic activity

Column name	Average	Max	Min	SD	Sum
Unicolumn statistics: training set					
−log (% inhibition)	−1.8050	−1.0980	−1.9920	0.3123	−25.2700
Unicolumn statistics: test set					
−log (% inhibition)	−1.6910	−1.2380	−1.9830	0.3480	−11.8370

(C5), 146.18 (C3), 141.14 (C–Ar), 138.54 (C–Ar), 137.81 (C–Ar), 137.25 (C–Ar), 136.69 (C–Ar), 130.25 (2C, C–Ar), 130.08 (C–Ar), 128.92 (2C, C–Ar), 128.21 (2C, C–Ar), 127.92 (2C, C–Ar), 121.05 (C–Ar), 120.42 (C–Ar), 117.82 (C–Ar), 117.40 (C–Ar), 103.46 (C4), 21.15 (CH3). LCMS *m/z* $[M]^+$ 388.16. Anal. Calcd. for $C_{26}H_{20}N_4$ (388.46): C, 80.39; H, 5.19; N, 14.42. Found: C, 80.88; H, 5.20; N, 14.42.

Pharmacology

The anticonvulsant studies of the synthesized compounds were conducted as per National Institute of Neurological and Communicative Disorders and Stroke (NINDS) guidelines (Roger *et al.*, 1984), at Animal house of Pacific College of Pharmacy, PAHER University, Udaipur, having institutional animal ethical committee with Registration no. 1622/PO/a/12/CPCSEA.

The profile of anticonvulsant activity of final compounds **7–27** was established in the MES and scPTZ tests, after intraperitoneal (i.p.) injection in mice at doses of 30, 100, and 300 mg/kg. For each compound, the animals were divided into three groups for three different doses, each group consisting of six animals. An observation was carried out at two different time intervals—0.5 and 4 h.

In the *MES screen*, an electrical stimulus of 0.2 s in duration (150 mA in rats) is delivered via corneal electrodes primed with an electrolyte solution containing an anesthetic agent. The end point is the tonic extension of the hind limbs. In the control (i.p. saline) groups, the procedures cause immediate hind limb tonic extension. Rats not displaying hind limb tonic extension were considered to be protected from seizures. The % inhibition of duration of tonic extensor phase was calculated for each animal for the purpose of comparison of results.

The *scPTZ test* utilizes a dose of pentylenetetrazole (85 mg/kg in mice) that produces clonic seizures lasting for a period of at least 5 s in 97 % (CD_{97}) of animals tested. PTZ is administered 0.5 and 4 h after injections of tested compounds, and observation is carried out for 30 min. In the control groups, the first episode of clonic convulsions is observed between 6 and 15 min of observation. The absence of clonic convulsions in the observed time period of 0.5 and 4 h is interpreted as the compound's ability to protect against PTZ-induced seizures.

Furthermore, in addition to the primary anticonvulsant screening, the *acute neurological toxicity (NT)* was determined in mice by the rotarod test and in rats by positional sense test.

To find out the statistical significance, the results of each group of animals were compared with that of control with the help of Student's paired *t* test. The value of $P < 0.05$ was considered to be statistically significant.

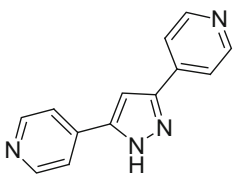

Fig. 9 3,5-Dipyridinyl-*1H*-pyrazole nucleus as the template for the alignment

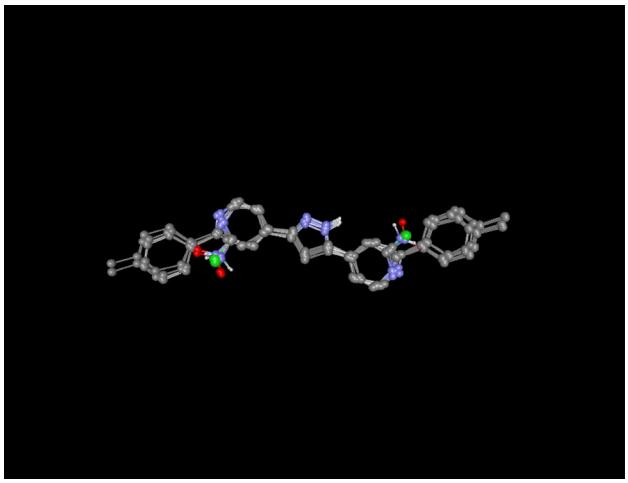

Fig. 10 Alignment of molecules for the development of 3D QSAR models through KNN-MFA

QSAR

2D QSAR

All the synthesized compounds were subjected to 2D QSAR analysis via three different regression methods, viz., multiple linear regression, principal component regression, and partial least square regression methods to obtain the statistically best model.

Table 7 Unicolumn statistics of selected training and test sets for 3D QSAR model development of compound for antiepileptic activity

Column name	Average	Max	Min	SD	Sum
Unicolumn statistics: training set					
−log (% inhibition)	−1.8050	−1.0980	−1.9920	0.3123	−25.2700
Unicolumn statistics: test set					
−log (% inhibition)	−1.6910	−1.2380	−1.9830	0.3480	−11.8370

The structures were constructed using the 2D draw application and were converted to 3D structures. Energy minimization and geometry optimization was conducted using Merck molecular force field (MMFF) method with root mean square (RMS) gradient set to 0.01 and iteration limit to 10,000. The 2D descriptors (physicochemical and alignment independent) were calculated for the optimized compounds, and the invariable descriptors (the descriptors that are constant for all the molecules) were removed as they do not contribute to QSAR. The manual selection of test and training set was done in the approximate ratio of 1: 3 according to Golbraikh and Tropsha (2002) which resulted in models with statistically better predictive power than by random selection method. Accordingly for each biological activity, seven compounds were selected as test set and remaining 14 compounds as training set. Calculation of unicolumn statistics (Table 6) further reflected the right selection of test and training sets as shown in each section of activity below.

The above showed that the test set is interpolative, i.e., derived within the minimum–maximum range of the training set. The average and standard deviation of the training and test sets provides insight into the relative difference in mean and point density distribution (along mean) of the two sets. In each of the cases below, mean in the test set is higher than the training set shows the presence of relatively more active molecules as compared to the inactive ones. Also, the similar standard deviation in both the sets in each case indicates that the spread in both the set with their respective mean is comparable.

All the 21 compounds were subjected to regression analysis using MLR, PCR, and PLS as model-building methods coupled with stepwise variable selection. QSAR equations were generated by using −1og % inhibition values as dependent variable and various descriptor values as independent variables. Regression analysis was carried out and the best model cross-validated. Cross-correlation limit was set as 0.5, number of variable in final equation as 5, and term selection criteria as r^2, F-test "in" as 4 and F-test "out" as 3.99. Variance cutoff was set to 0 and scaling as autoscaling, number of random iteration was set to 10.

3D QSAR

Alignment of all the 21 compounds was done using template-based alignment, where a template structure (Fig. 9) was defined and used as a basis for the alignment of a set of molecules; the aligned structures (Fig. 10) were used for 3D QSAR study.

The electrostatic and steric descriptors were calculated for given biological data (−log % inhibition) of the compounds. For calculation of field descriptor values, both electrostatic and steric field types with cutoffs 10.0 and 30.0 kcal/mol, respectively, were selected, and charge type was selected as Gasteiger–Marsili. Dielectric constant was set to 1.0 considering the distance-dependent dielectric function. Probe setting was carbon atom with charge 1.0 and grid setting as follows:

	From	To	Interval
X	−10.115	24.0225	2.0000
Y	0.306657	14.2794	2.0000
Z	−4.0000	4.0000	2.0000

This resulted in the calculation of 2080 field descriptors (1040 for each electrostatic and steric) for all the compounds in separate columns. The invariable columns were removed from the work sheet. The optimal test and training data sets were generated using manual method as done for 2D QSAR analysis. The method resulted in selection and seven compounds as test set and remaining 14 as training set.

The set data was observed for activity distribution through unicolumn statistics (Table 7) which revealed that almost all the compounds in test set are within the minimum–maximum limit of the training set.

Building QSAR models by KNN-MFA Since these were a large pool of descriptors available to build model, various variable selection methods were used along with k-nearest neighborhood (KNN) to find optimal subset of descriptors for KNN-MFA model, viz., stepwise variable selection, simulated annealing, and genetic algorithm.

For stepwise forward–backward method, the cross-correlation limit was set to 0.5 and term selection criteria as q^2. *F*-test "in" was set to 4.0 and *F*-test "out" to 3.99. As some additional parameters, variance cutoff was set as 2 kcal/mol Å and scaling and autoscaling, additionally the K-nearest neighbor parameter setting was done within the range of 2–5 and prediction method was selected as distance-based weighted average.

For simulated annealing as variable selection method, the cross-correlation limit was set as 0.5, terms in model as 4, maximum temperature as 100, minimum temperature as 0.01, iteration at given temperature as 5, decrease temperature by as 10, seed as 0, perturbation limit as 1, and term selection criteria as q^2.

For the development of models through GA, the GA parameter settings included cross-correlation limit as 0.5, crossover probability as 0.95, mutation probability as 0.05, term selection criteria as q^2, population as 10, no. of generations 10,000, print after iterations 100, and seed as 0. Convergence criteria 0.01, convergence ending criteria 5, and chromosome length as 3. Additional parameter settings were described in stepwise variable selection method.

Conclusion

In conclusion, the present project gave the library of 21 new 3,5-bipyridinyl-*1H*-pyrazole derivatives with seven compounds having good antiepileptic potential against maximum electroshock (MES) convulsions. The SAR and QSAR studies revealed that the anticonvulsant activity of pyrazolyl pyridines was related with the substituents on pyridyl as well as pyrazole moiety. Two important conclusions from 2D QSAR analysis were as follows: First, the electronic character of substituent in the present set of the compound was less important than bulk of the same, and second, a smaller molecule substituted at 3-position on pyrazole and 8- and/or 17-position(s) of pyridine would give rise to more effective anticonvulsant agents. Result of 3D QSAR analysis was also in accordance with the results of pharmacological screening as the range of steric and electrostatic fields at the mentioned points suggested the bulk and electronic character of the substituent at that position. Two important conclusions drawn from 3D QSAR analysis were as follows: Compounds having substitution on pyridine moieties with an atom or group having the same electrostatic potential would be less active while pyridyl substitutions with different electronic characters would favor the activity. Second, bulk is important for entrance into binding pocket of the receptor; compounds with bulky substituents on both the pyridyl moieties were found to be detrimental for the activity, for a compound to be a better anticonvulsant, either of the pyridyl moieties must have a smaller substituent having electronic character as suggested by 3D QSAR result. Thus, it can be concluded that the nucleus 3,5-bipyridinyl-1*H*-pyrazole itself is the pharmacophoric site of the molecule and by taking clues from models obtained through 2D and 3D QSAR analysis, new, better anticonvulsant agents can be developed.

Acknowledgments Authors are highly thankful to sophisticated analytical instrument facility (SAIF), Punjab University, Chandigarh, India, for spectrophotometric and elemental analyses. We are also grateful to Mr. Neeraj Kumar Kamra, Asst. Professor, Geetanjali Institute of Pharmacy, Udaipur, Rajasthan, India, for his support during the project.

Compliance with ethical standards

Conflict of interest The authors declare no conflict of interest.

References

Ajmani S, Jadhav K, Kulkarni SA (2006) Three-dimensional QSAR using the K-nearest neighbor method and its interpretation. J Chem Inf Model 46:24–31

Armijo JA, Shushtarian M, Valdizan EM, Cuadrado A, de las Cuevas I, Adín J (2005) Ion channels in epilepsy. Curr Pharm Des 11(15):1975–2003

Bialer M, Johannessen SI, Kupferberg HJ, Levy RH, Perucca E, Tomson T (2007) Progress report on new antiepileptic drugs: a summary of the eight Eilat conference (EILAT VIII). Epilepsy Res 73(1):1–52

Bruno-Blanch L, Galvez J, Garcia-Domenach R (2003) Topological virtual screening: a way to find new anticonvulsant drugs from chemical diversity. Bioorg Med Chem Lett 13(16):2749–2754

Golbraikh A, Tropsha A (2002) Predictive QSAR modeling based on diversity sampling of experimental datasets for the training and test set selection. J Comput Aided Mol Des 16(5–6):357–369

Heller ST, Natarajan SR (2006) 1, 3-Diketones from acid chlorides and ketones: a rapid and general one pot synthesis of pyrazoles. Org Lett 8(13):2675–2678

Hou T, Xu X (2001) Three-dimensional quantitative structure activity relationship analysis of some cinnamamides. Chemom Intell Lab 56:123–132

Krogsgaard-Larsen P, Liljefors T, Ulf Madsen (2002) Textbook of drug design and discovery. Taylor and Francis, London, p 554

Lien EJ, Tong GL, Chou JT, Lien LL (1973) Structural requirements for centrally acting drugs I. J Pharm Sci 62(2):246–250

Löscher W, Schmidt D (2002) New horizons in the development of antiepileptic drug. Epilepsy Res 50:3–16

Malawska B (2005) New anticonvulsant agents. Curr Top Med Chem 5(1):69–85

Marder M, Estiu G, Blanch LB, Viola H, Wasowski C, Medina JH (2001) Molecular modelling and QSAR analysis of the interaction of flavone derivatives with the benzodiazepine site of $GABA_A$ receptor complex. Bioorg Med Chem 9:323–335

Marone S, Rozas I, Weaver DF (1999) Theoretical structural analyses of tricyclic neuroactive drugs: quantum pharmacologic descriptors for clustering anticonvulsant, antidepressant, and antipsychotic activities. J Mol Struct 467:25–30

Meldrum BS, Rogawski MA (2007) Molecular targets for antiepileptic drug development. Neurotherapeutics 4(1):18–61

Palluotto F, Carotti A, Casini G, Campagna F, Genchi G, Rizzo M, De Sarro GB (1996) Structure activity relationships of 2-aryl-

2,5dihydropyridazino [4,3-b]indol-3(3H)-ones at the benzodiazepine receptor. Bioorg Med Chem 4(Pt. 12):2091–2104

Pradhan J, Goyal A (2015) Synthesis of some nuclear substitution derivatives of 4-acetyl pyridine. Int J Pharm Chem Anal 2(3):113–119

Rogawski MA, Porter RJ (1990) Antiepileptic drugs: pharmacological mechanisms and clinical efficacy with consideration of promising developmental stage compounds. Pharmacol Rev 42(3):223–286

Roger JP, James JC, Gill DG, Bettie JH, Harvey JK, Barrett S, Billy GW (1984) Antiepileptic drug development program. Cleve Clin J Med 51(2):293–305

Subbareddy NS, Sinha S, Parthasarathy S (2014) Epilepsy: Indian perspective. Ann Indian Acad Neurol 17(Suppl 1):S3–S11

Vlife MDS software package, version 4.4, supplied by Vlife science technologies Pvt. Ltd, 1, Akshay 50, Anand park, Aundh, Pune, India 411007

Verli H, Albuquerque MG, Bicca de Alencastro R, Barreiro EJ (2002) Local intersection volume: a new 3D descriptor applied to develop a 3D-QSAR pharmacophore model for benzodiazepine receptor ligands. Eur J Med Chem 37(3):219–229

Wong MG, Defina JA, Andrews PR (1986) Conformational analysis of clinically active anticonvulsant drugs. J Med Chem 29(4):562–572